
SAMBO-RL: Shifts-aware Model-based Offline Reinforcement Learning

Wang Luo¹ Haoran Li¹ Zicheng Zhang¹ Congying Han¹ Jiayu Lv¹ Tiande Guo¹

Abstract

Model-based offline reinforcement learning trains policies using pre-collected datasets and learned environment models, eliminating the need for direct real-world environment interaction. However, this paradigm is inherently challenged by distribution shift (DS). Existing methods address this issue by leveraging off-policy mechanisms and estimating model uncertainty, but they often result in inconsistent objectives and lack a unified theoretical foundation. This paper offers a comprehensive analysis that disentangles the problem into two fundamental components: model bias and policy shift. Our theoretical and empirical investigations reveal how these factors distort value estimation and restrict policy optimization. To tackle these challenges, we derive a novel Shifts-aware Reward (SAR) through a unified probabilistic inference framework, which modifies the vanilla reward to refine value learning and facilitate policy training. Building on this, we introduce Shifts-aware Model-based Offline Reinforcement Learning (SAMBO-RL), a practical framework that efficiently trains classifiers to approximate SAR for policy optimization. Empirical experiments show that SAR effectively mitigates DS, and SAMBO-RL achieves superior or comparable performance across various benchmarks, underscoring its effectiveness and validating our theoretical analysis.

1. Introduction

Offline reinforcement learning (RL) (Lange et al., 2012; Levine et al., 2020) learns policies from the offline dataset generated by a behavior policy, avoiding additional online interaction with the environment. This approach shows remarkable potential in data-driven decision scenarios (Emerson et al., 2023; Sinha et al., 2022) where exploration is costly or hazardous. The model-based framework (Luo

et al., 2018) is particularly effective for offline RL (Yu et al., 2020; 2021; Sun et al., 2023; Li et al., 2024). It involves learning models of the environment from the offline dataset and utilizing these models to generate data for policy training. However, directly learning a policy using offline and synthetic data introduces the distribution shift challenge. This shift causes the training objective to deviate from the true objective of RL, leading to poor test performance.

Prior methods in model-based offline RL focus on directly leveraging off-policy methods in online RL and heuristic model uncertainty for conservative learning to mitigate the impact of distribution shift. For instance, MOPO (Yu et al., 2020) uses the predicted variance of the learned model as an uncertainty penalty on rewards. MOBILE (Sun et al., 2023) penalizes value learning of model data according to the uncertainty of the Bellman Q-function estimated by ensemble models. RAMBO (Rigter et al., 2022) considers the trajectory distribution in the worst case and adversarially trains the policy and transition model while ensuring accurate predictions. However, these approaches have resulted in a biased training objective due to the model uncertainty and remain the distribution shift problem to be solved.

In this paper, we demystify the distribution shift problem in model-based RL and study its fundamental properties. We first show that this problem arises from both model bias and policy shift, and further analyze their impacts on policy optimization. Unlike the heuristic descriptions of model uncertainty, model bias fundamentally characterizes the inconsistency between the learned model and actual environment dynamics in predicting subsequent states. This bias leads to inaccurate estimations of trajectory returns, resulting in distorted objectives. If the learned model overestimates or underestimates the probability of generating a trajectory, it consequently causes the overestimation or underestimation of trajectory returns. Additionally, policy shift depicts the changes in state-action visitation distribution caused by the deviation between the learned policy π and behavior policy π_b . This shift implicitly forces π towards π_b , hindering the learning process and slowing down policy convergence. In contrast, previous studies heuristically mitigate these two issues from off-policy algorithms and model uncertainty.

To address these challenges, we theoretically derive adjustments for model bias and policy shift by employing a

¹School of Mathematical Sciences, University of Chinese Academy of Sciences, Beijing, China. Correspondence to: Congying Han <hancy@ucas.ac.cn>.

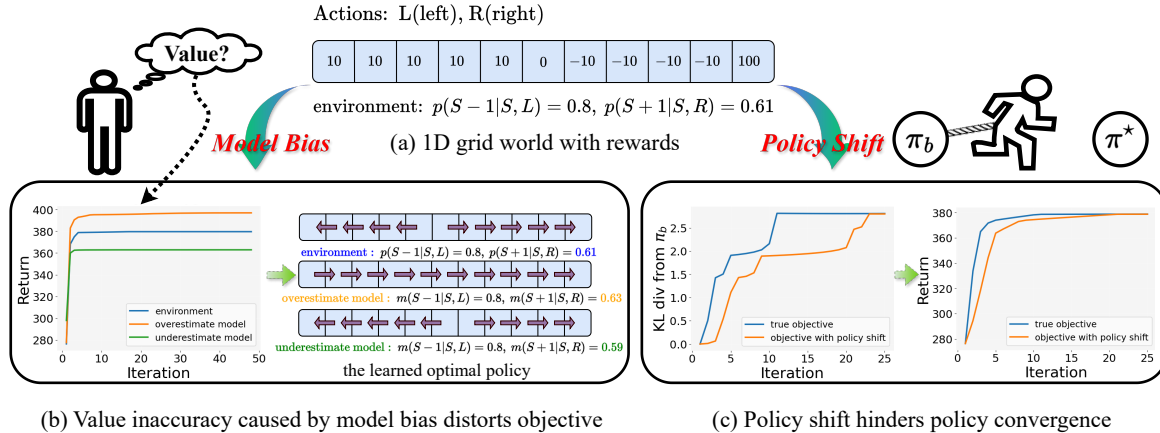


Figure 1. The negative impacts of model bias and policy shift. (a) In the 1D grid world, the agent can take two actions: move left (L) or move right (R) from the current state S to the adjacent grid cells $S-1$ or $S+1$, with movement obstructed at the boundaries. The initial state is uniformly distributed, and the agent receives undiscounted rewards upon reaching specific states. (b) The left panel illustrates value estimates during training and the final policy convergence with and without model bias. Even slight model bias can significantly distort value function estimates, leading the learned policies to deviate from the true optimal policy in the actual environment. (c) The right panel showcases expected returns and the KL divergence between the learned policy π and the behavior policy π_b during training with and without policy shift. We find that policy shift implicitly restricts π to remain close to π_b , thereby slowing policy convergence.

unified probabilistic inference framework, and introduce a shifts-aware reward, which integrates the vanilla reward with adjustments for model bias and policy shift. The model bias adjustment penalizes the reward to mitigate issues of overestimation or underestimation, thereby refining value learning and preventing its convergence to local optima. Meanwhile, the policy shift modification revises the reward to motivate π to escape the limitation of π_b , accelerating policy convergence. Building upon our theoretical framework, we develop Shifts-aware Model-based Offline Reinforcement Learning (SAMBO-RL). This approach incorporates model bias adjustment for model-generated data and policy shift modification for offline data. Furthermore, it learns a transition classifier and action classifiers to approximate the shifts-aware reward and then performs policy optimization based on this adjusted reward. Our contributions include:

- We demystify the distribution shift problem in model-based offline RL, *i.e.*, model bias distorts the estimation of the value function, while policy shift imposes an implicit policy limitation that hinders policy convergence.
- We upgrade the vanilla reward into a shifts-aware reward incorporating model bias adjustment and policy shift modification. This modified reward is used for policy learning to mitigate distribution shift in model-based offline RL.
- We devise SAMBO-RL, which trains transition and action classifiers to approximate the shifts-aware reward, effectively addressing both model bias and policy shift.
- We show that shifts-aware reward effectively mitigates distribution shift, and SAMBO-RL demonstrates superior or comparable performance across various benchmarks.

2. Related Work

Model-free Offline RL encompasses two primary approaches: policy constraints and value regularization, both incorporating conservatism (Jin et al., 2021). Policy constraint methods aim to keep the learned policy close to the behavioral policy, mitigating distribution shift. For instance, BEAR (Kumar et al., 2019) and BRAC (Wu et al., 2019) constrain the learned policy by minimizing different divergences. BCQ (Fujimoto et al., 2019) perturbs actions during learning to ensure they remain within the action space of the offline dataset by learning a generative model of the behavior policy. On the other hand, value regularization methods add conservative regularization terms to the value optimization objective, avoiding out-of-distribution (OOD) actions. CQL (Kumar et al., 2020) penalizes the Q-values of OOD samples by incorporating regularization into the value loss function. TD3+BC (Fujimoto & Gu, 2021) introduces a behavior cloning regularization into the TD3 (Fujimoto et al., 2018) objective. Similarly, EDAC (An et al., 2021) and PBRL (Bai et al., 2021) penalize the Q-function based on uncertainty derived from an ensemble of Q-networks. MCQ (Lyu et al., 2022) actively trains OOD actions by constructing pseudo-target values to alleviate over-pessimism.

Model-based Offline RL approximates the environment using learned models and performs conservative policy optimization (Lu et al., 2021), achieving high data efficiency (Li et al., 2024). MOPO (Yu et al., 2020) incorporates conservatism by penalizing rewards based on the uncertainty of model predictions. MOREL (Kidambi et al., 2020) introduces a pessimistic MDP to penalize rewards of state-action pairs in unexplored regions. COMBO (Yu et al., 2021) ex-

tends CQL to the model-based setting, regularizing the value function on OOD samples. TT (Janner et al., 2021) uses a transformer to model offline trajectories and employs beam search for planning. RAMBO (Rigter et al., 2022) adopts an adversarial approach, training policy and model within a robust framework while ensuring accurate transition predictions of the model. CBOP (Jeong et al., 2022) adaptively weights multi-step returns in a model-based value expansion framework (Feinberg et al., 2018). Lastly, MOBILE (Sun et al., 2023) introduces penalties during value learning by leveraging the uncertainty of the Bellman Q-function estimates derived from ensemble learned dynamic models.

3. Preliminaries

MDP. We focus on a Markov decision process (MDP) specified by the tuple $M = (\mathcal{S}, \mathcal{A}, p, r, \mu_0, \gamma)$, where \mathcal{S} denotes the state space, \mathcal{A} denotes the action space, $p(s'|s, a)$ is the environment transition dynamics, positive $r(s, a) > 0$ is the reward function, $\mu_0(s)$ is the initial state distribution, and $\gamma \in (0, 1)$ is the discount factor. Given an MDP, we define the state value function $V^\pi(s) = \mathbb{E}_{\pi, p} [\sum_{t=0}^{\infty} \gamma^t r(s_t, a_t) | s_0 = s]$ and the Q function $Q^\pi(s, a) = \mathbb{E}_{\pi, p} [\sum_{t=0}^{\infty} \gamma^t r(s_t, a_t) | s_0 = s, a_0 = a]$.

MBPO. Similar to previous works (Yu et al., 2020; 2021; Rigter et al., 2022; Sun et al., 2023), we focus on model-based policy optimization (MBPO) (Janner et al., 2019), which employs an actor-critic RL algorithm. MBPO first performs k -step rollouts using the model $m(s'|s, a)$ starting from state $s \in \mathcal{D}_{env}$ and adds the generated data to a replay buffer \mathcal{D}_m . Then it optimizes the policy using mini-batches of data sampled from $\mathcal{D}_{env} \cup \mathcal{D}_m$, where each datapoint is sampled from the real dataset \mathcal{D}_{env} with probability f and the model dataset \mathcal{D}_m with probability $1 - f$.

Trajectory Formulation. To demystify the distribution shift, We consider the trajectory formulation of optimization objectives. Let $p^\pi(\cdot)$ represent the probability distribution over trajectories $\mathcal{H} = \{\tau = (s_0, a_0, r_0, s_1, \dots)\}$ generated by executing policy π under dynamics p . This is given by:

$$p^\pi(\tau) = \mu_0(s_0) \prod_{t=0}^{\infty} p(s_{t+1}|s_t, a_t) \pi(a_t|s_t). \quad (1)$$

The training data \mathcal{D}_{train} can be interpreted as being generated by a data collection policy π_c through rollouts in dynamics q . Consequently, the probability of observing trajectory τ in the training data can be formulated as $q^{\pi_c}(\tau)$. The reinforcement learning objective and the practical training objective are then formalized as the following equations:

$$\mathcal{J}_M(\pi) = \mathbb{E}_{\tau \sim p^\pi} [R(\tau)] \text{ and } \mathcal{J}(\pi) = \mathbb{E}_{\tau \sim q^{\pi_c}} [R(\tau)], \quad (2)$$

where $R(\tau) = \sum_{t=0}^{\infty} \gamma^t r(s_t, a_t)$ represents the discounted return of the whole trajectory $\tau = (s_0, a_0, r_0, s_1, \dots)$.

4. Shifts-aware Policy Optimization

We first formalize the distribution shift problem as shift weighting and further delve into its negative effects on policy optimization from theory and experiments. To address these challenges, we employ probabilistic inference to derive a surrogate objective and formulate a shifts-aware reward. Finally, we implement this theoretical framework within model-based offline RL and introduce SAMBO-RL, a practical algorithm designed to mitigate distribution shifts.

4.1. Demystifying Distribution Shift

We examine the distribution shift problem from an optimization perspective and identify its origins as model bias and policy shift. Then we explore how these factors affect accuracy in value estimation and impose implicit policy restrictions, resulting in a biased objective and slow convergence. The supplementary analysis is in Appendix A.1.

Shift Weighting. The training objective $\mathcal{J}(\pi)$ in (2) can be expressed as the following trajectory formulation:

$$\mathcal{J}(\pi) = \mathbb{E}_{\tau \sim p^\pi(\tau)} \left[\frac{q^{\pi_c}(\tau)}{p^\pi(\tau)} R(\tau) \right]. \quad (3)$$

Compared to (2), it indicates that for a given trajectory τ , the true objective under practical sampling distributions differs in shift weighting $\frac{q^{\pi_c}(\tau)}{p^\pi(\tau)}$ from the training objective, which formalizes the distribution shift in trajectory formulation.

Substituting (1) into the shift weighting $\frac{q^{\pi_c}(\tau)}{p^\pi(\tau)}$, we can attribute this weighting to two primary components: model bias and policy shift, reformulated as the following:

$$\frac{q^{\pi_c}(\tau)}{p^\pi(\tau)} = \underbrace{\prod_t \frac{q(s_{t+1}|s_t, a_t)}{p(s_{t+1}|s_t, a_t)}}_{\text{model bias}} \underbrace{\prod_t \frac{\pi_c(a_t|s_t)}{\pi(a_t|s_t)}}_{\text{policy shift}}. \quad (4)$$

Model bias illustrates the discrepancy between the dynamics used for training and those of the actual environment, while policy shift represents the divergence between the policies used for sampling training data and those being learned.

Negative Impact of Shift Weighting. We analyze the impact of shift weighting from model bias and policy shift.

(i) To illustrate the effect of model bias, we examine the scenario where the training policy π operates within model dynamics q , which diverges from the actual environment dynamics p . In this context, the training objective $\mathcal{J}(\pi)$ is:

$$\mathcal{J}(\pi) = \mathbb{E}_{\tau \sim p^\pi} \left[R(\tau) \prod_{t=0}^{\infty} \frac{q(s_{t+1}|s_t, a_t)}{p(s_{t+1}|s_t, a_t)} \right].$$

Compared to the true objective (3), the compounded prediction bias of the model significantly affects value estimation

and leads to a distorted objective. Specifically, when the model q overestimates or underestimates the probability of generating trajectory τ , it consequently overestimates or underestimates the expected return of this trajectory in the real environment. This essentially introduces bias for the optimization objective, resulting in wrong training directions.

(ii) To delve deeper into the policy optimization process under policy shift, we consider the setting where a sampling policy π_c is executed within the true environment transition dynamics p . In this scenario, the training objective $\mathcal{J}(\pi)$ is:

$$\mathcal{J}(\pi) = \mathbb{E}_{(s,a) \sim d^{p,\pi}} \left[r(s,a) \frac{d^{p,\pi_c}(s,a)}{d^{p,\pi}(s,a)} \right].$$

Here, $d^{p,\pi}(s,a)$ is the state-action visitation distribution under dynamics p and policy π , i.e. $d^{p,\pi}(s,a) = (1 - \gamma) \mathbb{E}_{s_0 \sim \mu_0, s_t \sim p, a_t \sim \pi} [\sum_{t=0}^{\infty} \gamma^t \mathbb{I}(s_t = s, a_t = a)]$, where \mathbb{I} represents the indicator function. Note that π_c is related to π . Compared to the true objective, the policy shift implicitly forces policy π to approach π_c , hindering the learning process and slowing down policy convergence. Specifically, for a state-action pair (s,a) associated with a high reward, ideal policy updates should increase $\pi(a|s)$. However, if the currently learned policy π adequately approximates the optimal policy and satisfies $d^{p,\pi}(s,a) > d^{p,\pi_c}(s,a)$, the reward for (s,a) can be underestimated. This situation could even prompt policy updates to decrease $\pi(a|s)$, contrary to the optimal direction. Similarly, for the state-action pair (s,a) with a low reward, if the currently π is reasonably good and leads to $d^{p,\pi}(s,a) < d^{p,\pi_c}(s,a)$, the reward can be overestimated, potentially resulting in policy updates to increase $\pi(a|s)$ that do not align with optimal policy directions.

Toy Examples. To empirically validate our analysis of model bias and policy shift, we use a 1D grid world example, as depicted in Fig. 1 (a). In Fig. 1 (b), we compare the training process with and without model bias and find the value function overestimation and underestimation under model bias. These results reveal that even slight deviations in model dynamics can significantly distort value function estimates, leading to a biased training objective. Consequently, the policies learned by the agents deviate from the optimal policy. To assess the impact of the policy shift, we examine a model-free offline setting where data is pre-collected using a behavior policy π_b . Fig. 1 (c) showcases that the KL divergence between the learned policy π and π_b under policy shift is substantially reduced compared to the scenario without policy shift, sometimes even decreasing undesirably. This indicates that policy shift does compel π to align closely with π_b , thereby impeding the training process and substantially slowing down the policy convergence.

4.2. Shifts-aware Reward via Probabilistic Inference

This subsection introduces a novel shifts-aware reward through a unified probabilistic inference framework, serving

as a lower-bound surrogate for the true objective. We examine how this modified reward contributes to refining the value function and motivating π to escape the limitations of behavior policy, thus mitigating model bias and policy shift.

Shifts-aware Reward. We introduce the shifts-aware reward $\tilde{r}(s_t, a_t, s_{t+1})$ formulated within trajectories. It comprises the vanilla reward, adjustments for model bias, and modifications for policy shift, expressed as the following:

$$\begin{aligned} \tilde{r}(s_t, a_t, s_{t+1}) &= \log r(s_t, a_t) \\ &+ \frac{1}{(1-\gamma)\gamma^t} \left[\log \frac{p(s_{t+1}|s_t, a_t)}{q(s_{t+1}|s_t, a_t)} + \log \frac{\pi(a_t|s_t)}{\pi_c(a_t|s_t)} \right]. \end{aligned} \quad (5)$$

This modified reward forms the basis of our surrogate objective function during training, which is formulated as:

$$\mathcal{L}(\pi) = \mathbb{E}_{q^{\pi_c}(\tau)} \left[\sum_{t=0}^{\infty} \gamma^t \tilde{r}(s_t, a_t, s_{t+1}) \right]. \quad (6)$$

Additionally, we establish that $\mathcal{L}(\pi)$ serves as a lower bound for the true objective, ensuring its rationality as a surrogate.

Theorem 4.1. *Let $\mathcal{L}(\pi)$ be the training objective defined in (6) and \tilde{r} denote the shifts-aware reward (5). Then,*

$$\log [\mathcal{J}_M(\pi)] \geq (1-\gamma)\mathcal{L}(\pi), \quad \forall \pi.$$

Optimization objective based on this shifts-aware reward provides a methodological foundation for integrating shift adjustments seamlessly into reinforcement learning algorithms to uniformly address model bias and policy shift.

Modal Bias Adjustment. We now examine how this adjustment refines the value estimation and addresses the challenge of model bias. By rolling out the learned policy π within the model dynamics m , we obtain a model-generated dataset \mathcal{D}_m . Furthermore, the modified training objective of the model dataset \mathcal{D}_m can be computed as the following:

$$\begin{aligned} \tilde{J}(\pi) &= \mathbb{E}_{s \sim \mathcal{D}_m, a \sim \pi(\cdot|s), s' \sim \mathcal{D}_m} [\tilde{r}(s, a, s')] \\ &= \mathbb{E}_{(s,a) \sim \mathcal{D}_m} [\log r(s, a) - \alpha D_{\text{KL}}(m(\cdot|s, a) \| p(\cdot|s, a))]. \end{aligned}$$

This modified reward consists of the logarithmic vanilla reward penalized by the KL divergence between the model and environment dynamics. This adjustment reduces value function misestimations by accounting for the accuracy of the learned model, encouraging the development of both a high-return policy and an accurate model approximation.

Policy Shift Modification. To delve into the positive effect of policy shift modification, we consider a dataset \mathcal{D}_b generated by executing the behavior policy π_b within the environment p . Moreover, the modified training objective of the dataset \mathcal{D}_b is derived as the following formulation:

$$\begin{aligned} \tilde{J}(\pi) &= \mathbb{E}_{s \sim \mathcal{D}_b, a \sim \pi(\cdot|s), s' \sim \mathcal{D}_b} [\tilde{r}(s, a, s')] \\ &= \mathbb{E}_{s \sim \mathcal{D}_b} [\mathbb{E}_{a \sim \pi(\cdot|s)} [\log r(s, a)] + \beta D_{\text{KL}}(\pi(\cdot|s) \| \pi_b(\cdot|s))], \end{aligned}$$

which introduces a bonus to the vanilla reward based on the KL divergence between π and π_b . This modification guides π to break out of the confines of the behavior policy π_b , promoting better exploration and more effective learning.

4.3. Shifts-aware Model-based Offline RL

We apply the shifts-aware reward in model-based offline RL and develop the practical framework, SAMBO-RL.

To adapt the shifts-aware reward for practical implementation, where training data is typically stored in transition format rather than trajectories, we introduce two weighting factors, α and β . These factors replace the respective coefficients in the reward function, shaping it as the following:

$$\tilde{r}(s, a, s') = \log r(s, a) + \alpha \log \frac{p(s'|s, a)}{q(s'|s, a)} + \beta \log \frac{\pi(a|s)}{\pi_c(a|s)}.$$

These weighting factors ensure the reward and adjustments are properly balanced in transition-based learning scenarios, which is empirically validated in the following experiments.

Furthermore, since the environment dynamics p and behavior policy π_b are typically unknown and cannot be exactly computed, we derive two classifiers to estimate the shifts-aware reward (Eysenbach et al., 2020; 2022). Details are shown in Appendix A.3. Specifically, these classifiers estimate model bias adjustment $\log \frac{p(s'|s, a)}{q(s'|s, a)}$ and policy shift modification $\log \frac{\pi(a|s)}{\pi_c(a|s)}$ respectively. The transition classifier $C_\phi(s, a, s')$ estimates the probability that the transition (s, a, s') comes from the environment, while the action classifier $C_\psi(s, a)$ estimate the probability that a given state-action pair (s, a) is generated by the current policy π .

We train the classifiers by minimizing the loss functions:

$$\mathcal{L}(\varphi) = -\mathbb{E}_{\mathcal{D}_1}[\log C_\varphi] - \mathbb{E}_{\mathcal{D}_2}[\log(1 - C_\varphi)]. \quad (7)$$

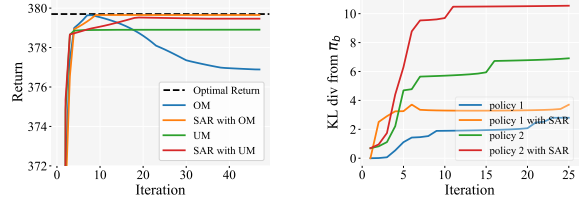
For the transition classifier $C_\phi = C_\phi(s, a, s')$, $\mathcal{D}_1 = \mathcal{D}_{env}$ is the offline dataset, and $\mathcal{D}_2 = \mathcal{D}_m$ is the model-generated dataset. For the action classifier $C_\psi = C_\psi(s, a)$, $\mathcal{D}_1 = \mathcal{D}_\pi$ is the dataset collected by executing the current policy π , and $\mathcal{D}_2 = \mathcal{D}_{env}$ is the offline dataset. Based on these classifiers, we approximate the shifts-aware reward as the following:

$$\begin{aligned} \tilde{r}(s, a, s') &\approx \log r(s, a) \\ &+ \alpha \log \frac{C_\phi(s, a, s')}{1 - C_\phi(s, a, s')} + \beta \log \frac{C_\psi(s, a)}{1 - C_\psi(s, a)}. \end{aligned} \quad (8)$$

The complete procedure of SAMBO-RL is outlined in Algorithm 1, with further details provided in Appendix B.

5. Experiments

In our experiments, we focus on three objectives: (1) validating the effectiveness of shifts-aware reward, (2) comparing



(a) Model Bias Adjustment (b) Policy Shift Modification

Figure 2. Assessment of the shifts-aware reward. (a) Model bias adjustment mitigates inaccuracies in value estimation, achieving a nearly optimal return. (b) Policy shift modification addresses implicit policy restrictions, leading to faster convergence.

the performance of SAMBO with previous methods, and (3) analyzing the contribution of each component and hyperparameter within SAMBO to its overall performance.

We evaluate our algorithm using standard offline RL benchmarks in Mujoco environments and conduct an ablation study to assess its performance. Our implementation is based on the OfflineRL-Kit library¹, a comprehensive and high-performance library for implementing offline reinforcement learning algorithms. The basic parameters of our algorithm are consistent with the settings in this library.

5.1. Effectiveness of Shifts-aware Reward

We conduct an evaluation of the effectiveness of the shifts-aware Reward in addressing model bias and policy shift issues within the 1D grid world illustrated in Fig. 1 (a).

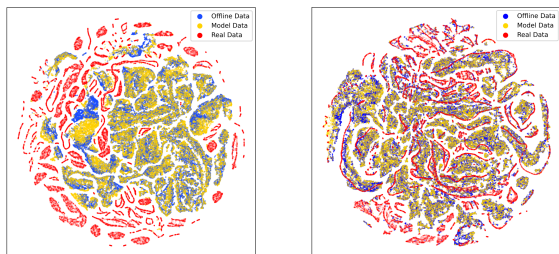
Model Bias Adjustment. Model bias exacerbates inaccuracies in value estimates, ultimately resulting in a distorted optimization objective. To evaluate the effects of model bias adjustment on the training process, we conduct experiments. As illustrated in Fig. 2 (a), we execute the policy gradient algorithm under four settings: using the vanilla reward with the overestimating model (OM) or underestimating model (UM), the shifts-aware reward with the overestimating model (SAR with OM) underestimating model (SAR with UM). We then evaluate the expected return of the learned policy after each training update in the actual environment. The results show that while the OM initially achieves optimal returns, it rapidly diverges from the optimal policy. In contrast, SAR with OM effectively counters the performance degradation caused by model overestimation, sustaining optimal returns. Similarly, SAR with UM mitigates the policy suboptimality due to model underestimation, achieving a return near the theoretical optimum.

Policy Shift Modification. Policy shift implicitly restricts policy updates. To assess the efficacy of the policy shift modification, we apply the policy gradient algorithm to the offline objective $\mathcal{J}(\pi) = \mathbb{E}_{s \sim d^{p, \pi_b}} [V^\pi(s)]$ in the environment depicted in Fig. 1 (a). We test four settings: the vanilla

¹<https://github.com/yihaosun1124/OfflineRL-Kit>

Table 1. Results on the D4RL Gym benchmark. MOPO’s results are obtained on the “v0” datasets; MOPO*’s results are obtained from experiments in the OfflineRL-Kit library on the “v2” datasets. The numbers reported for SAMBO are the normalized scores averaged over the final iteration of training across 4 seeds, with \pm standard deviation. The top three scores are highlighted in bold. We use an asterisk “*” for the best score, an underscore “_” for the second, and bold text for the third.

Task Name	BC	CQL	TD3+BC	EDAC	MOPO	MOPO*	COMBO	TT	RAMBO	MOBILE	SAMBO (Ours)
halfcheetah-random	2.2	31.3	11.0	28.4	35.4	38.5	38.8	6.1	39.5	39.3	39.7*±2.0
hopper-random	3.7	5.3	8.5	25.3	11.7	31.7	17.9	6.9	25.4	31.9	32.4*±0.5
walker2d-random	1.3	5.4	1.6	16.6	13.6	7.4	7.0	5.9	0.0	17.9*	8.1 ± 7.8
halfcheetah-medium	43.2	46.9	48.3	65.9	42.3	72.4	54.2	46.9	77.9*	74.6	72.5±3.8
hopper-medium	54.1	61.9	59.3	101.6	28.0	62.8	97.2	67.1	87.0	106.6*	99.7±0.3
walker2d-medium	70.9	79.5	83.7	92.5*	17.8	84.1	81.9	81.3	84.9	87.7	78.3±2.6
halfcheetah-medium-replay	37.6	45.3	44.6	61.3	53.1	72.1*	55.1	44.1	68.7	71.7	70.6±1.6
hopper-medium-replay	16.6	86.3	60.9	110.0*	67.5	92.7	89.5	99.4	99.5	103.9	101.5±1.5
walker2d-medium-replay	20.3	76.8	81.8	87.1	39.0	85.9	56.0	82.6	89.2	89.9	92.3*±1.5
halfcheetah-medium-expert	44.0	95.0	90.0	106.3	63.3	83.6	90.0	95.0	95.4	108.2*	97.8 ±0.3
hopper-medium-expert	53.9	96.9	98.0	110.7	23.7	74.6	111.0	110.0	88.2	112.6*	111.0 ±1.2
walker2d-medium-expert	90.1	109.1	110.1	114.7	44.6	108.2	103.3	101.9	56.7	115.2*	106.1 ± 2.9



(a) MOBILE

(b) SAMBO

Figure 3. The (s, a, s') distributions of offline RL algorithms result in the Hopper-M task. Model Data represents the distribution of data generated by executing the final learned policy in the dynamic model, while Real Data represents the distribution of data generated by executing the final learned policy in the environment.

reward or SAR, combined with a behavior policy that is either uniformly distributed or the opposite of the optimal policy. We measure the KL divergence between the learned policy and the behavior policy after each update. As illustrated in Fig. 2 (b), the algorithm using the vanilla reward is limited by the behavior policy, serving a lower KL divergence and slower convergence. In contrast, the algorithm employing the SAR effectively motivates policy to be optimistic. It overcomes the restriction, displaying a higher and more stable divergence and achieving faster convergence.

Effectiveness in Complex Tasks. We also conducted experiments on complex tasks. Fig. 3 shows a visual comparison in the NeoRL task (details in Sec. 5.2.2). SAMBO effectively constrains model-generated data (i.e., Model Data) to align closely with the Offline Data, whereas the previous state-of-the-art method, MOBILE, imposes weaker constraints. Furthermore, the real-world data (i.e., Real Data) generated by SAMBO is well-aligned with the Offline Data and remains tightly concentrated, indicating the SAMBO’s

effectiveness. In contrast, the Real Data from MOBILE deviates significantly from both the Offline and Model Data, still suffering from distribution shift, leading to diminished performance. We attribute this discrepancy to SAMBO’s robust handling of model bias and policy shift, ensuring that the Real Data, Model Data, and Offline Data remain closely aligned, effectively mitigating the distribution shift.

5.2. Benchmark Results

5.2.1. D4RL

Datasets. In line with prior research, SAMBO is evaluated using the D4RL benchmark (Fu et al., 2020) on the MuJoCo simulator (Todorov et al., 2012). The evaluation encompasses 12 datasets spanning three environments (halfcheetah, hopper, walker2d) and four dataset types (random, medium, medium-replay, medium-expert). The “v2” versions of datasets are employed for assessment.

Baselines. We evaluate SAMBO against several baseline methods, including model-free methods such as BC (Bain & Sammut, 1995; Ross et al., 2011), which learns the behavior policy, CQL (Kumar et al., 2020), TD3+BC (Fujimoto & Gu, 2021), and EDAC (An et al., 2021), as well as model-based methods such as MOPO (Yu et al., 2020), COMBO (Yu et al., 2021), TT (Janner et al., 2021), RAMBO (Rigter et al., 2022), and MOBILE (Sun et al., 2023).

Comparison Results. Results are presented in Table 1. Each number represents the normalized score, calculated as $100 \times (\text{score} - \text{random policy score}) / (\text{expert policy score} - \text{random policy score})$ (Fu et al., 2020). SAMBO achieves strong performance on random datasets and demonstrates competitive performance across medium, medium-replay, and medium-expert datasets. This performance aligns with our theoretical analysis. By addressing both model bias and

Table 2. Normalized average returns in NeoRL benchmark over 4 random seeds. The results for MOBILE are reported from the original paper, and MOBILE* represents the results obtained by executing the official implementation.

Task Name	BC	CQL	TD3+BC	EDAC	MOPO	MOBILE	MOBILE*	SAMBO (Ours)
HalfCheetah-L	29.1	38.2	30.0	31.3	40.1	54.7	54.8	39.8 ± 2.6
Hopper-L	15.1	16.0	15.8	18.3	6.2	17.4	18.2	19.4 ± 1.3
Walker2d-L	28.5	44.7	43.0	40.2	11.6	37.6	23.7	46.1 ± 5.7
HalfCheetah-M	49.0	54.6	52.3	54.9	62.3	77.8	79.0	62.5 ± 1.6
Hopper-M	51.3	64.5	70.3	44.9	1.0	51.1	43.4	67.6 ± 12.2
Walker2d-M	48.7	57.3	58.6	57.6	39.9	62.2	60.1	63.4 ± 4.0
HalfCheetah-H	71.3	77.4	75.3	81.4	65.9	83.0	71.8	71.6 ± 13.9
Hopper-H	43.1	76.6	75.3	52.5	11.5	87.8	42.3	93.9 ± 15.2
Walker2d-H	72.6	75.3	69.6	75.5	18.0	74.9	71.9	79.2 ± 0.6

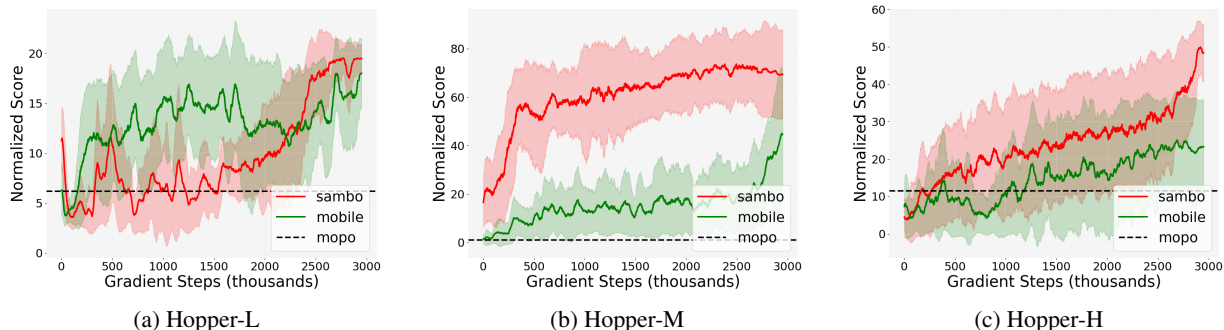


Figure 4. Performance comparison of Hopper tasks in NeoRL benchmark.

policy shift, SAMBO effectively balances the exploitation of offline data with the need to overcome the limitations of the behavioral policy. This approach enables the algorithm to be more aggressive and optimistic in its search for the optimal policy. In scenarios involving low-quality datasets, the aggressive exploration of SAMBO is more likely to yield benefits, potentially leading to the discovery of a superior policy. Conversely, a conservative approach may impede the learning of optimal policy in such contexts. For high-quality datasets, the advantages of aggressive exploration tend to diminish. Fortunately, in these scenarios, methods that emphasize estimating Q-value uncertainty perform effectively. This suggests that our approach and conservative estimation methods can perform well on complementary datasets.

5.2.2. NEORL

Datasets. NeoRL (Qin et al., 2022) is a benchmark designed to emulate real-world scenarios by generating datasets through a more conservative policy, aligning closely with real-world data-collection scenarios. The datasets, characterized by their narrow scope and limited coverage, present a substantial challenge for offline RL algorithms. In this work, we examine nine datasets across three environments (HalfCheetah-v3, Hopper-v3, Walker2d-v3) and three dataset quality levels (L, M, H), corresponding to low, medium, and high-quality datasets. NeoRL offers different

numbers of trajectories for each task (100, 1000, and 10000), and we consistently selected 1000 trajectories in our test.

Baselines. We compare SAMBO with baseline methods that align with the d4rl experiments in Section 5.2.1, excluding TT, COMBO, and RAMBO, as no results for these methods are reported in their original papers or the NeoRL paper, and determining suitable hyperparameters for them would require an excessive amount of computational time.

Comparison Results. Results are presented in Table 2 and Figure 4. We compare the learning curves of model-based approaches in the NeoRL benchmark. Since MOPO does not have an official implementation on NeoRL, we report its score based on the original NeoRL paper. The experiments show that Our algorithm achieves superior or competitive performance on the more challenging and realistic NeoRL datasets, which can be seen as lower-quality datasets compared to the D4RL datasets. In particular, SAMBO demonstrates exceptional performance in the Walker2d and Hopper environments, which, in contrast to the HalfCheetah environment, exhibit higher control complexity, more intricate action dimensions, and greater training difficulty. These offline datasets more accurately capture the dynamic control challenges encountered in real-world scenarios, making them significantly demanding and highlighting that SAMBO has strong potential for real-world applications. More experiments and discussions are provided in Appendix D.3.

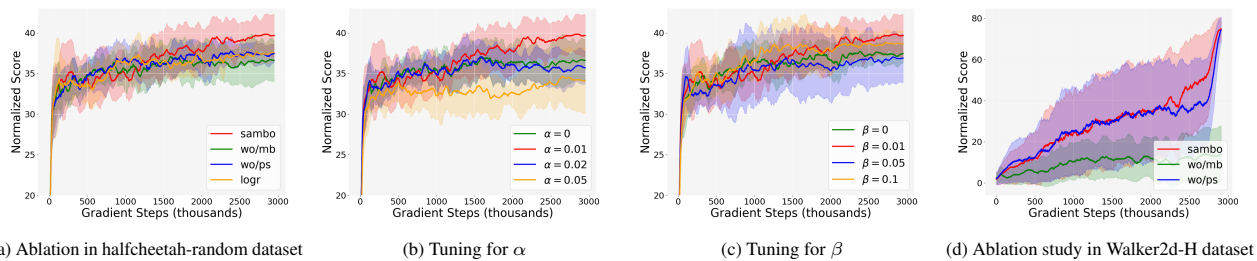


Figure 5. Illustration of hyperparameter experiments in D4RL benchmark and NeoRL benchmark. (a) and (d) The effectiveness of model bias adjustment and policy shift modification in the shifts-aware reward. (b) A large model bias adjustment coefficient α increases conservativeness. (c) A large policy shift modification coefficient β increases the aggressiveness of exploration.

5.3. Ablation Studies

We conducted ablation studies on our method to understand why SAMBO demonstrates competitive performance. The following experimental results are presented in Figure 5.

Ablation. Our shifts-aware reward integrates both the model bias adjustment and the policy shift modification. To elucidate the importance of these components, we perform ablation studies on the Halfcheetah-random task in D4RL benchmark and Walker2d-H task in NeoRL benchmark. As shown in Figure 5 (a) and (d), we assess the performance under four configurations: SAMBO, SAMBO without model bias adjustment (wo/mb), SAMBO without policy shift modification (wo/ps), and SAMBO without any modifications (logr), while keeping all other parameters consistent.

Figure 5 (a) show that, compared to the experiment denoted as logr, the performance of wo/mb deteriorates. This degradation arises because wo/mb employs policy shift modification to break the implicit limitations of the behavior policy and encourage more aggressive exploration. However, it does not address model bias, resulting in significant inaccuracies in value estimation, ultimately leading to suboptimal performance. This negative effect is particularly evident in the narrow Walker2d-H dataset, as seen in Figure 5 (d). Conversely, the wo/ps ablation addresses model bias but neglects policy shift adjustments. While this reduces value misestimation, the algorithm remains constrained by the behavior policy due to the lack of policy shift modification. Consequently, wo/ps is less effective in discovering a more optimal policy. As shown in Figure 5 (a), the performance of wo/ps is inferior to sambo, and Figure 5 (d) illustrates that wo/ps converges slowly compared to sambo. In contrast, SAMBO incorporates not only model bias adjustment but also policy shift modification, facilitating aggressive exploration while addressing value estimation challenges, thus alleviating suboptimal performance.

Hyperparameter Tuning. SAMBO is primarily regulated by two key hyperparameters: the model bias adjustment coefficient α and the policy shift modification coefficient β . The model bias adjustment coefficient α adjusts model-

generated data, with larger values overly penalizing exploration and smaller values inducing over-optimism, both harming performance. To validate this, we fixed $\beta = 0.01$ and varied α in the halfcheetah task. As shown in Fig. 5 (b), increasing α from 0 to 0.05 initially improves performance but later hinders it due to excessive conservativeness, highlighting the need for a balanced α in policy learning.

The policy shift coefficient β regulates modifications to offline data, controlling deviation from the behavior policy. Larger β values enhance exploration by encouraging greater deviation from the behavior policy, but also increase the risk of unsafe or suboptimal actions. As shown in Fig. 5 (c), the algorithm exhibits performance fluctuations as β increases from 0 to 0.1. Low β may lead to suboptimal solutions, while high β can induce excessive aggressiveness and instability. Therefore, β also needs to be set appropriately.

6. Conclusion and Discussion

In this paper, we analyze the distribution shift problem, attributing its root causes to model bias and policy shift. Model bias results in distorted objectives, while policy shift obstructs the convergence of policies. We introduce a shifts-aware policy optimization framework to uniformly address these challenges through shift-aware rewards (SAR) and apply it within the model-based offline setting, thereby proposing our SAMBO-RL algorithm. Notably, our framework is versatile and can be integrated into general reinforcement learning algorithms. Our main limitation is classifier accuracy; imprecise classifiers struggle to estimate the shifts-aware reward accurately, leading to unstable training. In future work, We aim to explore alternative methods that directly address distribution shifts using datasets, thereby eliminating the need for classifier estimation. Additionally, we will extend our shifts-aware reward framework to tackle distribution shift challenges in online settings, with a particular focus on policy shift problems. Our novel analysis and results related to policy shifts in this context open new avenues for better exploiting offline datasets and overcoming the implicit restrictions imposed by behavior policies.

Impact Statement

This study addresses the distribution shift problem in offline model-based reinforcement learning (RL), with the potential to facilitate the deployment of RL algorithms in real-world applications, particularly in scenarios where data collection is expensive. The research aims to enhance the robustness and reliability of RL systems in real world. However, the direct deployment of RL systems in high-risk domains, such as autonomous driving, may introduce substantial risks, especially if algorithms fail to adapt to unforeseen distribution shifts in real-world environments. Furthermore, the application of offline RL models, particularly in sensitive areas like healthcare, may raise significant ethical concerns. In such domains, the training data may not fully represent all patient groups. If distribution shift issues are not adequately addressed, the resulting treatment policies may fail for certain patient populations. Therefore, to ensure the safe, effective, and equitable deployment of RL systems in real world, rigorous testing, validation, and continuous monitoring are essential.

References

- An, G., Moon, S., Kim, J.-H., and Song, H. O. Uncertainty-based offline reinforcement learning with diversified q-ensemble. *Advances in neural information processing systems*, 34:7436–7447, 2021.
- Bai, C., Wang, L., Yang, Z., Deng, Z.-H., Garg, A., Liu, P., and Wang, Z. Pessimistic bootstrapping for uncertainty-driven offline reinforcement learning. In *International Conference on Learning Representations*, 2021.
- Bain, M. and Sammut, C. A framework for behavioural cloning. In *Machine Intelligence 15*, pp. 103–129, 1995.
- Emerson, H., Guy, M., and McConville, R. Offline reinforcement learning for safer blood glucose control in people with type 1 diabetes. *Journal of Biomedical Informatics*, 142:104376, 2023.
- Eysenbach, B., Asawa, S., Chaudhari, S., Levine, S., and Salakhutdinov, R. Off-dynamics reinforcement learning: Training for transfer with domain classifiers. *arXiv preprint arXiv:2006.13916*, 2020.
- Eysenbach, B., Khazatsky, A., Levine, S., and Salakhutdinov, R. R. Mismatched no more: Joint model-policy optimization for model-based rl. *Advances in Neural Information Processing Systems*, 35:23230–23243, 2022.
- Feinberg, V., Wan, A., Stoica, I., Jordan, M. I., Gonzalez, J. E., and Levine, S. Model-based value estimation for efficient model-free reinforcement learning. *arXiv preprint arXiv:1803.00101*, 2018.
- Fu, J., Kumar, A., Nachum, O., Tucker, G., and Levine, S. D4rl: Datasets for deep data-driven reinforcement learning. *arXiv preprint arXiv:2004.07219*, 2020.
- Fujimoto, S. and Gu, S. S. A minimalist approach to offline reinforcement learning. *Advances in neural information processing systems*, 34:20132–20145, 2021.
- Fujimoto, S., Hoof, H., and Meger, D. Addressing function approximation error in actor-critic methods. In *International conference on machine learning*, pp. 1587–1596. PMLR, 2018.
- Fujimoto, S., Meger, D., and Precup, D. Off-policy deep reinforcement learning without exploration. In *International conference on machine learning*, pp. 2052–2062. PMLR, 2019.
- Janner, M., Fu, J., Zhang, M., and Levine, S. When to trust your model: Model-based policy optimization. *Advances in neural information processing systems*, 32, 2019.
- Janner, M., Li, Q., and Levine, S. Offline reinforcement learning as one big sequence modeling problem. *Advances in neural information processing systems*, 34: 1273–1286, 2021.
- Jeong, J., Wang, X., Gimelfarb, M., Kim, H., Abdulhai, B., and Sanner, S. Conservative bayesian model-based value expansion for offline policy optimization. *arXiv preprint arXiv:2210.03802*, 2022.
- Jin, Y., Yang, Z., and Wang, Z. Is pessimism provably efficient for offline rl? In *International Conference on Machine Learning*, pp. 5084–5096. PMLR, 2021.
- Kidambi, R., Rajeswaran, A., Netrapalli, P., and Joachims, T. Morel: Model-based offline reinforcement learning. *Advances in neural information processing systems*, 33: 21810–21823, 2020.
- Kumar, A., Fu, J., Soh, M., Tucker, G., and Levine, S. Stabilizing off-policy q-learning via bootstrapping error reduction. *Advances in neural information processing systems*, 32, 2019.
- Kumar, A., Zhou, A., Tucker, G., and Levine, S. Conservative q-learning for offline reinforcement learning. *Advances in Neural Information Processing Systems*, 33: 1179–1191, 2020.
- Lange, S., Gabel, T., and Riedmiller, M. Batch reinforcement learning. In *Reinforcement learning: State-of-the-art*, pp. 45–73. Springer, 2012.
- Levine, S., Kumar, A., Tucker, G., and Fu, J. Offline reinforcement learning: Tutorial, review, and perspectives on open problems. *arXiv preprint arXiv:2005.01643*, 2020.

- Li, G., Shi, L., Chen, Y., Chi, Y., and Wei, Y. Settling the sample complexity of model-based offline reinforcement learning. *The Annals of Statistics*, 52(1):233–260, 2024.
- Lu, C., Ball, P. J., Parker-Holder, J., Osborne, M. A., and Roberts, S. J. Revisiting design choices in offline model-based reinforcement learning. *arXiv preprint arXiv:2110.04135*, 2021.
- Luo, Y., Xu, H., Li, Y., Tian, Y., Darrell, T., and Ma, T. Algorithmic framework for model-based deep reinforcement learning with theoretical guarantees. *arXiv preprint arXiv:1807.03858*, 2018.
- Lyu, J., Ma, X., Li, X., and Lu, Z. Mildly conservative q-learning for offline reinforcement learning. *Advances in Neural Information Processing Systems*, 35:1711–1724, 2022.
- Qin, R.-J., Zhang, X., Gao, S., Chen, X.-H., Li, Z., Zhang, W., and Yu, Y. Neorl: A near real-world benchmark for offline reinforcement learning. *Advances in Neural Information Processing Systems*, 35:24753–24765, 2022.
- Rigter, M., Lacerda, B., and Hawes, N. Rambo-rl: Robust adversarial model-based offline reinforcement learning. *Advances in neural information processing systems*, 35:16082–16097, 2022.
- Ross, S., Gordon, G., and Bagnell, D. A reduction of imitation learning and structured prediction to no-regret online learning. In *Proceedings of the fourteenth international conference on artificial intelligence and statistics*, pp. 627–635. JMLR Workshop and Conference Proceedings, 2011.
- Sinha, S., Mandlekar, A., and Garg, A. S4rl: Surprisingly simple self-supervision for offline reinforcement learning in robotics. In *Conference on Robot Learning*, pp. 907–917. PMLR, 2022.
- Sun, Y., Zhang, J., Jia, C., Lin, H., Ye, J., and Yu, Y. Model-bellman inconsistency for model-based offline reinforcement learning. In *International Conference on Machine Learning*, pp. 33177–33194. PMLR, 2023.
- Todorov, E., Erez, T., and Tassa, Y. Mujoco: A physics engine for model-based control. In *2012 IEEE/RSJ international conference on intelligent robots and systems*, pp. 5026–5033. IEEE, 2012.
- Wu, Y., Tucker, G., and Nachum, O. Behavior regularized offline reinforcement learning. *arXiv preprint arXiv:1911.11361*, 2019.
- Yu, T., Thomas, G., Yu, L., Ermon, S., Zou, J. Y., Levine, S., Finn, C., and Ma, T. Mopo: Model-based offline policy optimization. *Advances in Neural Information Processing Systems*, 33:14129–14142, 2020.
- Yu, T., Kumar, A., Rafailov, R., Rajeswaran, A., Levine, S., and Finn, C. Combo: Conservative offline model-based policy optimization. *Advances in neural information processing systems*, 34:28954–28967, 2021.

A. Theoretical Analysis

A.1. The Supplement Analysis of Distribution Shift

Dual Formulation of Model Bias. The reinforcement learning optimization objective can be equivalently reformulated in its dual form, expressed as $\mathcal{J}_M(\pi) = \mathbb{E}_{(s,a) \sim d^{p,\pi}}[r(s,a)]$, where $d^{p,\pi}(s,a)$ denotes the state-action visitation distribution under dynamics p and policy π . To illustrate the impact of model bias in the dual formulation, we similarly examine the scenario where the training policy π is applied within the model dynamics q . The training objective $\mathcal{J}(\pi)$ is derived as follows:

$$\mathcal{J}(\pi) = \mathbb{E}_{(s,a) \sim d^{q,\pi}}[r(s,a)] = \mathbb{E}_{(s,a) \sim d^{p,\pi}}[r(s,a) \frac{d^{q,\pi}(s,a)}{d^{p,\pi}(s,a)}].$$

Model bias can result in inaccuracies in estimating the state-action visitation distribution, subsequently affecting the accuracy of value function estimation. Similarly, if the learned model overestimates or underestimates the state-action visitation distribution, it will lead to corresponding overestimations or underestimations of rewards, thereby distorting the objective.

Trajectory Formulation of Policy Shift. Similarly, we consider the trajectory formulation of policy shift. We execute the sampling policy π_c within the environment transition dynamics p . Then the training objective $\mathcal{J}(\pi)$ is then given by:

$$\mathcal{J}(\pi) = \mathbb{E}_{\tau \sim p^{\pi_c}}[R(\tau)] = \mathbb{E}_{\tau \sim p^{\pi}} \left[R(\tau) \prod_{t=0}^{\infty} \frac{\pi_c(a_t | s_t)}{\pi(a_t | s_t)} \right].$$

The policy shift can influence the value estimation of trajectories, imposing implicit constraints on policy learning. For a high-reward trajectory τ , if the current policy π closely approximates the optimal policy and satisfies $\prod_t \pi(a_t | s_t) > \prod_t \pi_c(a_t | s_t)$, it may lead to an underestimation of the return for trajectory τ . Conversely, for a low-reward trajectory τ , if the current policy is relatively effective and satisfies $\prod_t \pi(a_t | s_t) < \prod_t \pi_c(a_t | s_t)$, this can result in an overestimation of the return for trajectory τ . Both of these impede the effective learning of the policy.

A.2. The Proof of Theorem 1

Theorem A.1. Let $\mathcal{L}(\pi)$ be the training objective defined in (6) and \tilde{r} denote the shifts-aware reward (5). Then,

$$\log[\mathcal{J}_M(\pi)] \geq (1 - \gamma)\mathcal{L}(\pi), \quad \forall \pi.$$

Proof. The cumulative discounted reward $R(\tau)$ of trajectory $\tau = (s_0, a_0, r_0, s_1, \dots)$ can be written as:

$$R(\tau) = \sum_{t=0}^{\infty} \gamma^t r(s_t, a_t) = \frac{1}{1 - \gamma} \sum_{t=0}^{\infty} (1 - \gamma) \gamma^t r(s_t, a_t). \quad (9)$$

As discussed in the main text, the probability distribution over a trajectory τ can be formulated as follows:

$$p^{\pi}(\tau) = \mu_0(s_0) \prod_{t=0}^{\infty} p(s_{t+1} | s_t, a_t) \pi(a_t | s_t), \quad q^{\pi_c}(\tau) = \mu_0(s_0) \prod_{t=0}^{\infty} q(s_{t+1} | s_t, a_t) \pi_c(a_t | s_t). \quad (10)$$

Then according to (9) and (10) and Jensen's inequality, we have

$$\begin{aligned}
 \log [\mathcal{J}_M(\pi)] &= \log \mathbb{E}_{p^\pi(\tau)} R(\tau) \\
 &= \log \mathbb{E}_{q^{\pi_c}(\tau)} \left[R(\tau) \frac{p^\pi(\tau)}{q^{\pi_c}(\tau)} \right] \\
 &= \log \mathbb{E}_{q^{\pi_c}(\tau)} \left[R(\tau) \frac{\mu(s_0) \prod_{t=0}^{\infty} p(s_{t+1}|s_t, a_t) \pi(a_t|s_t)}{\mu(s_0) \prod_{t=0}^{\infty} q(s_{t+1}|s_t, a_t) \pi_c(a_t|s_t)} \right] \\
 &\geq \mathbb{E}_{q^{\pi_c}(\tau)} \left[\log R(\tau) + \sum_{t=0}^{\infty} \left(\log \frac{p(s_{t+1}|s_t, a_t)}{q(s_{t+1}|s_t, a_t)} + \log \frac{\pi(a_t|s_t)}{\pi_c(a_t|s_t)} \right) \right] \\
 &\geq \mathbb{E}_{q^{\pi_c}(\tau)} \left[\log \frac{1}{1-\gamma} + \sum_{t=0}^{\infty} (1-\gamma)\gamma^t \log r(s_t, a_t) + \sum_{t=0}^{\infty} \left(\log \frac{p(s_{t+1}|s_t, a_t)}{q(s_{t+1}|s_t, a_t)} + \log \frac{\pi(a_t|s_t)}{\pi_c(a_t|s_t)} \right) \right] \\
 &\geq \mathbb{E}_{q^{\pi_c}(\tau)} \left[\sum_{t=0}^{\infty} \left((1-\gamma)\gamma^t \log r(s_t, a_t) + \log \frac{p(s_{t+1}|s_t, a_t)}{q(s_{t+1}|s_t, a_t)} + \log \frac{\pi(a_t|s_t)}{\pi_c(a_t|s_t)} \right) \right] \\
 &= (1-\gamma) \mathbb{E}_{q^{\pi_c}(\tau)} \left[\sum_{t=0}^{\infty} \gamma^t \left(\log r(s_t, a_t) + \frac{1}{(1-\gamma)\gamma^t} \left(\log \frac{p(s_{t+1}|s_t, a_t)}{q(s_{t+1}|s_t, a_t)} + \log \frac{\pi(a_t|s_t)}{\pi_c(a_t|s_t)} \right) \right) \right] \\
 &= (1-\gamma) \mathcal{L}(\pi).
 \end{aligned}$$

□

A.3. Classifiers Estimation Derivations

We assume that all steps in the derivation are appropriate, that the denominator is non-zero, and that the argument of the logarithm is not zero.

A.3.1. TRANSITION CLASSIFIER DERIVATION.

Define two events \mathbb{E} and \mathbb{M} , where

$\mathbb{E} = \{\text{Given the state-action pair } (s_t, a_t), \text{ the agent interacts with the environment } p \text{ to generate the subsequent state.}\},$

$\mathbb{M} = \{\text{Given the state-action pair } (s_t, a_t), \text{ the agent interacts with the model } q \text{ to generate the subsequent state.}\}.$

The transition classifier is defined as $C_\phi(s_t, a_t, s_{t+1}) = P(\mathbb{E}|s_t, a_t, s_{t+1})$. Then

$$\begin{aligned}
 C_\phi(s, a, s_{t+1}) &= P(\mathbb{E}|s_t, a_t, s_{t+1}) = \frac{P(\mathbb{E}, s_t, a_t) P(s_{t+1}|s_t, a_t, \mathbb{E})}{P(s_t, a_t, s_{t+1})} \\
 &= \frac{P(\mathbb{E}|s_t, a_t) P(s_{t+1}|s_t, a_t, \mathbb{E})}{P(s_t, a_t) P(s_t, a_t, s_{t+1})}.
 \end{aligned} \tag{11}$$

Events \mathbb{E} and \mathbb{M} form a partition of the probability space, which means that

$$P(\mathbb{M}|s_t, a_t, s_{t+1}) = 1 - P(\mathbb{E}|s_t, a_t, s_{t+1}) = 1 - C_\phi(s, a, s_{t+1}).$$

Similarly, we have

$$\begin{aligned}
 1 - C_\phi(s, a, s_{t+1}) &= \frac{P(\mathbb{M}, s_t, a_t) P(s_{t+1}|s_t, a_t, \mathbb{M})}{P(s_t, a_t, s_{t+1})} \\
 &= \frac{P(\mathbb{M}|s_t, a_t) P(s_{t+1}|s_t, a_t, \mathbb{M})}{P(s_t, a_t) P(s_t, a_t, s_{t+1})}.
 \end{aligned} \tag{12}$$

According to (11) and (12), we have

$$\frac{C_\phi(s, a, s_{t+1})}{1 - C_\phi(s, a, s_{t+1})} = \frac{P(s_{t+1}|s_t, a_t, \mathbb{E}) P(\mathbb{E}|s_t, a_t)}{P(s_{t+1}|s_t, a_t, \mathbb{M}) P(\mathbb{M}|s_t, a_t)}. \tag{13}$$

Specifically, $P(s_{t+1}|s_t, a_t, \mathbb{E}) = p(s_{t+1}|s_t, a_t)$, where p represents the environment transition dynamic; $P(s_{t+1}|s_t, a_t, \mathbb{M}) = q(s_{t+1}|s_t, a_t)$, where q denotes the model transition dynamic. Then taking the logarithm of both sides of (13), we obtain:

$$\log \frac{C_\phi(s, a, s_{t+1})}{1 - C_\phi(s, a, s_{t+1})} = \log \frac{p(s_{t+1}|s_t, a_t)}{q(s_{t+1}|s_t, a_t)} + \log \frac{P(\mathbb{E}|s_t, a_t)}{P(\mathbb{M}|s_t, a_t)}. \quad (14)$$

Given the independence of the state-action pair (s_t, a_t) from the transition dynamics, we assume that the visit distribution of (s_t, a_t) remains identical. Then

$$\frac{P(\mathbb{E}|s_t, a_t)}{P(\mathbb{M}|s_t, a_t)} \approx \frac{d^\pi(s_t, a_t) |\mathcal{D}_{env}|}{d^\pi(s_t, a_t) |\mathcal{D}_m|} = \frac{|\mathcal{D}_{env}|}{|\mathcal{D}_m|}, \quad (15)$$

where $|\mathcal{D}_{env}|$ and $|\mathcal{D}_m|$ represent the sizes of the datasets \mathcal{D}_{env} and \mathcal{D}_m , respectively. Thus, $\frac{P(\mathbb{E}|s_t, a_t)}{P(\mathbb{M}|s_t, a_t)}$ can be approximated by a constant. Then according to (14) and (15), we have

$$\log \frac{p(s_{t+1}|s_t, a_t)}{q(s_{t+1}|s_t, a_t)} \approx \log \frac{C_\phi(s, a, s_{t+1})}{1 - C_\phi(s, a, s_{t+1})} - c_1,$$

where c_1 is a constant that does not influence the training of SAMBO.

A.3.2. ACTION CLASSIFIER DERIVATION.

The derivation of the action classifier is similar to that of the transition classifier. Define two events \mathbb{A} and \mathbb{C} , where

$$\mathbb{A} = \{\text{Given the state } s_t, \text{ the agent takes action } a_t \text{ according to policy } \pi\},$$

$$\mathbb{C} = \{\text{Given the state } s_t, \text{ the agent takes action } a_t \text{ according to the behavior policy } \pi_c\}.$$

The action classifier is defined as $C_{\psi_1}(s_t, a_t) = P(\mathbb{A}|s_t, a_t)$, Then

$$C_{\psi_1}(s, a) = P(\mathbb{A}|s_t, a_t) = \frac{P(a_t|s_t, \mathbb{A})P(\mathbb{A}|s_t)P(s_t)}{P(s_t, a_t)}, \quad (16)$$

$$1 - C_{\psi_1}(s, a) = P(\mathbb{C}|s_t, a_t) = \frac{P(a_t|s_t, \mathbb{C})P(\mathbb{C}|s_t)P(s_t)}{P(s_t, a_t)}. \quad (17)$$

Specifically, $P(a_t|s_t, \mathbb{A}) = \pi(a_t|s_t)$, $P(a_t|s_t, \mathbb{C}) = \pi_c(a_t|s_t)$. Then according to (16) and (17), we have

$$\frac{C_{\psi_1}(s, a)}{1 - C_{\psi_1}(s, a)} = \frac{\pi(a_t|s_t) P(\mathbb{A}|s_t)}{\pi_c(a_t|s_t) P(\mathbb{C}|s_t)}. \quad (18)$$

Similarly, $\frac{P(\mathbb{A}|s_t)}{P(\mathbb{C}|s_t)}$ can also be approximated by a classifier $C_{\psi_2}(s)$, i.e. $\frac{P(\mathbb{A}|s_t)}{P(\mathbb{C}|s_t)} = \frac{C_{\psi_2}(s)}{1 - C_{\psi_2}(s)}$. Thus, we can approximate $\frac{\pi(a_t|s_t)}{\pi_c(a_t|s_t)}$ using two classifiers,

$$\log \frac{\pi(a_t|s_t)}{\pi_c(a_t|s_t)} = \log \frac{C_{\psi_1}(s, a)}{1 - C_{\psi_1}(s, a)} - \log \frac{C_{\psi_2}(s)}{1 - C_{\psi_2}(s)}.$$

For simplicity, we use the notation

$$\log \frac{\pi(a_t|s_t)}{\pi_c(a_t|s_t)} = \log \frac{C_\psi(s, a)}{1 - C_\psi(s, a)}.$$

B. Implementation Details

We present a detailed outline of the SAMBO algorithm in Algorithm 1.

Algorithm 1 SAMBO-RL

Input: Offline dataset \mathcal{D}_{env} , learned dynamics models $\{m_\theta^i\}_{i=1}^N$, initialized policy π , shifts-aware reward hyperparameters α and β , rollout horizon h , rollout batch size b .

- 1: Train the probabilistic dynamics model $m_\theta(s', r|s, a) = \mathcal{N}(\mu_\theta(s, a), \Sigma_\theta(s, a))$ on \mathcal{D}_{env} .
- 2: Initialize the model dataset buffer $\mathcal{D}_m \leftarrow \emptyset$.
- 3: **for** $i = 1, 2, \dots, N_{iter}$ **do**
- 4: Initialize the policy dataset buffer $\mathcal{D}_\pi \leftarrow \emptyset$.
- 5: **for** $1, 2, \dots, b$ (in parallel) **do**
- 6: Sample state s_1 from \mathcal{D}_{env} for the initialization of the rollout.
- 7: **for** $j = 1, 2, \dots, h$ **do**
- 8: Sample an action $a_j \sim \pi(s_j)$.
- 9: Randomly pick dynamics m from $\{m_\theta^i\}_{i=1}^N$ and sample $s_{j+1}, r_j \sim m(s_j, a_j)$.
- 10: Add sample (s_j, a_j, r_j, s_{j+1}) to \mathcal{D}_m and \mathcal{D}_π .
- 11: **end for**
- 12: **end for**
- 13: Update classifiers C_ϕ and C_ψ according to Eq. (19) and Eq. (20), respectively.
- 14: Drawing samples from $\mathcal{D}_{env} \cup \mathcal{D}_m$, compute shifts-aware reward according to Eq. (21) and Eq. (22), respectively.
- 15: Run SAC with shifts-aware reward to update policy π .
- 16: **end for**

B.1. Model Training

In our approach, the model is represented by a probabilistic neural network that outputs a Gaussian distribution for both the next state and reward, given the current state and action:

$$m_\theta(s_{t+1}, r_t | s_t, a_t) = \mathcal{N}(\mu_\theta(s_t, a_t), \Sigma_\theta(s_t, a_t)).$$

Our model training approach is consistent with the methodology used in prior works (Janner et al., 2019; Yu et al., 2020). We train an ensemble of seven dynamics models and select the best five based on their validation prediction error from a held-out set containing 1000 transitions in the offline dataset \mathcal{D}_{env} . Each model in the ensemble is a 4-layer feedforward neural network with 200 hidden units. During model rollouts, we randomly choose one model from the best five models.

B.2. Classifiers Training

The transition classifier $C_\phi(s, a, s') \in [0, 1]$ represents the probability that the transition originated from the environment. It is trained by minimizing the standard cross-entropy loss function:

$$\mathcal{L}_\phi = -\mathbb{E}_{\mathcal{D}_{env}} [\log C_\phi(s, a, s')] - \mathbb{E}_{\mathcal{D}_m} [\log(1 - C_\phi(s, a, s'))]. \quad (19)$$

The action classifier $C_\psi(s, a) \in [0, 1]$ represents the probability that a given state-action pair (s, a) was generated by the current policy π . This classifier is trained by minimizing:

$$\begin{aligned} \mathcal{L}_{\psi_1} &= -\mathbb{E}_{\mathcal{D}_\pi} [\log C_{\psi_1}(s, a)] - \mathbb{E}_{\mathcal{D}_{env}} [\log(1 - C_{\psi_1}(s, a))], \\ \mathcal{L}_{\psi_2} &= -\mathbb{E}_{\mathcal{D}_\pi} [\log C_{\psi_2}(s)] - \mathbb{E}_{\mathcal{D}_{env}} [\log(1 - C_{\psi_2}(s))]. \end{aligned} \quad (20)$$

For data in the model dataset \mathcal{D}_m , the dynamics are governed by the model q . Furthermore, we approximate the training data collection policy for \mathcal{D}_m using the current policy π , i.e. $\pi_c = \pi$. Therefore, $\forall (s, a, r, s') \in \mathcal{D}_m$, the shifts-aware reward simplifies to

$$\tilde{r}(s, a, s') = \log r(s, a) + \alpha \log \frac{p(s'|s, a)}{q(s'|s, a)}.$$

Then, for all $(s, a, s') \in \mathcal{D}_m$, the shift-aware reward can be estimated using the following formulation,

$$\tilde{r}(s, a, s') \approx \log r(s, a) + \alpha \log \frac{C_\phi(s, a, s')}{1 - C_\phi(s, a, s')}. \quad (21)$$

For data in the offline dataset \mathcal{D}_{env} , the dynamics are governed by environment p , *i.e.* $q = p$, and the training data collection policy aligns with the behavioral policy, *i.e.* $\pi_c = \pi_b$. Therefore, $\forall (s, a, r, s') \in \mathcal{D}_{env}$, the shifts-aware reward simplifies to

$$\tilde{r}(s, a, s') = \log r(s, a) + \beta \log \frac{\pi(a|s)}{\pi_b(a|s)},$$

which is independent of the subsequent state s' . Then, for all $(s, a, s') \in \mathcal{D}_{env}$, the shift-aware reward can be estimated by

$$\tilde{r}(s, a, s') \approx \log r(s, a) + \beta \log \frac{C_\psi(s, a)}{1 - C_\psi(s, a)}. \quad (22)$$

B.3. Policy Learning

The policy optimization in our approach is based on the SAC algorithm, with hyperparameter configurations aligning with those employed in MOBILE (Sun et al., 2023). For each update, we draw a batch of 256 transitions, with 5% sourced from the offline dataset \mathcal{D}_{env} and the remaining 95% from the synthetic dataset \mathcal{D}_m . The detailed hyperparameter settings used for the D4RL benchmark are provided in Table 3.

Table 3. Hyperparameters for policy optimization in SAMBO

Hyperparameters	Value	Description
K	2	The number of critics.
γ	0.99	Discount factor.
l_r of actor	1×10^{-4}	Policy learning rate.
l_r of critic	3×10^{-4}	Critic learning rate.
Optimizer	Adam	Optimizers of the actor and critics.
f	0.05	Ratio of the real samples.
Batch size	256	Batch size for each update.
N_{iter}	3M	Total gradient steps.

C. Experimental Details

C.1. Benchmark

We conduct experiments on Gym tasks (“v2” version) within the D4RL (Fu et al., 2020) benchmark. We also evaluated SAMBO on the NeoRL (Qin et al., 2022) benchmark, a more challenging dataset generated using a more conservative policy to better reflect real-world data collection scenarios. These datasets are characterized by their narrow scope and limited coverage.

D4RL. We now provide the sources for the reported performance on this benchmark. For TD3+BC (Fujimoto & Gu, 2021), EDAC (An et al., 2021), TT (Janner et al., 2021), RAMBO (Rigter et al., 2022), and MOBILE (Sun et al., 2023), we cite the scores reported in the original papers, as these evaluations were conducted on the “v2” datasets in Gym. Since COMBO (Yu et al., 2021) does not provide source code, we include the results as reported in the original paper. The results of CQL (Kumar et al., 2020) are taken from the performance table in MOBILE, where CQL was retrained on the “v2” datasets in Gym. The results of MOPO* are obtained from experiments using the OfflineRL-Kit library² on the “v2” datasets. These scores are referenced in Table 1.

NeoRL. We report the performance of BC, CQL, and MOPO based on the original NeoRL paper, while the performance of TD3+BC, EDAC, and MOBILE is derived from the scores reported in the MOBILE (Sun et al., 2023) paper.

C.2. Hyperparameters

We list the hyperparameters that have been tuned as follows. The specific settings are detailed in Table 4 and Table 5.

²<https://github.com/yihaosun1124/OfflineRL-Kit>

Table 4. Hyperparameters of SAMBO used in the D4RL datasets.

Task Name	α	β	h	c
halfcheetah-random	0.01	0.01	5	-0.2
hopper-random	0.02	0.01	5	0
walker2d-random	0.3	0.3	5	0
halfcheetah-medium	0.03	0.03	5	0
hopper-medium	0.02	0.01	5	0
walker2d-medium	0.035	0.01	5	0
halfcheetah-medium-replay	0.01	0.01	5	0
hopper-medium-replay	0.05	0.05	5	0
walker2d-medium-replay	1	1	1	0
halfcheetah-medium-expert	0.3	0.3	5	0
hopper-medium-expert	1	1	5	0
walker2d-medium-expert	2	2	1	0

Table 5. Hyperparameters of SAMBO used in the NeoRL datasets.

Task Name	α	β	h	c
Halfcheetah-L	0.01	0.01	5	0
Hopper-L	0.3	0.3	5	0
Walker2d-L	3	1	1	0
Halfcheetah-M	0.1	0.1	5	0
Hopper-M	0.3	0.3	5	0
Walker2d-M	3	1	1	0
Halfcheetah-H	5	1	5	0
Hopper-H	0.3	0.3	5	0
Walker2d-H	3	1	1	0

Coefficient α and β . The model bias coefficient, α , determines the degree of correction for model bias, while the policy shift coefficient, β , regulates the extent of correction for policy shift.

Rollout Length h . Similar to MOPO, We perform short-horizon branch rollouts in SAMBO. we tune h in the range of $\{1, 5\}$ for Gym tasks in the D4RL benchmark.

Reward Truncation Coefficient c . To compute the logarithm of the reward term in the shifts-aware reward, we apply a translation to the real reward, which does not affect policy optimization. Specifically, given the offline dataset \mathcal{D}_{env} , let r_{max} denote the maximum reward and r_{min} denote the minimum reward in this dataset. Then we perform a translation and truncation on the real reward as follows:

$$r' = \min\{1 \times 10^{-8}, r - c(r_{max} - r_{min}) + 1 \times 10^{-8}\}.$$

Then we calculate the shifts-aware reward by

$$\tilde{r}(s, a, s') \approx \log r'(s, a) + \alpha \log \frac{C_\phi(s, a, s')}{1 - C_\phi(s, a, s')} + \beta \log \frac{C_\psi(s, a)}{1 - C_\psi(s, a)}.$$

In most datasets, we set $c = 0$. However, we observe that employing a negative value for c yields favorable results in certain datasets.

We terminate training at 1M to prevent potential performance degradation due to the rapid convergence of the HalfCheetah environment in NeoRL. Additionally, to maintain training stability in the HalfCheetah-high dataset, we freeze classifiers

after 0.5 million iterations. Similarly, in the walker2d-medium dataset of the D4RL benchmark, we ensure training stability by fixing the transition classifier after 1 million iterations.

C.3. Reward Function Discussion

Based on our derivation, if we start with $\mathbb{E}_{p^\pi(\tau)} e^{R(\tau)}$, we can obtain a new surrogate objective, which we refer to as SAMBO-r. In scenarios with sparse rewards and narrow datasets, where $\log r$ may distort the reward, SAMBO-r may be more suitable as a surrogate objective.

- **SAMBO.** The modified reward is

$$\tilde{r}(s, a, s') = \log r'(s, a) + \alpha \log \frac{C_\phi(s, a, s')}{1 - C_\phi(s, a, s')} + \beta \log \frac{C_\psi(s, a)}{1 - C_\psi(s, a)}.$$

- **SAMBO-r.** The modified reward is

$$\tilde{r}(s, a, s') = r'(s, a) + \alpha \log \frac{C_\phi(s, a, s')}{1 - C_\phi(s, a, s')} + \beta \log \frac{C_\psi(s, a)}{1 - C_\psi(s, a)}.$$

C.4. Computing Infrastructure

All experiments are conducted using a single GeForce GTX 3090 GPU and an Intel(R) Xeon(R) Gold 6330 CPU @ 2.00GHz. Our implementation code is based on the OfflineRL-Kit library. The software libraries and frameworks utilized in SAMBO are consistent with those specified in this library.

D. Omitted Experiments

D.1. Visualization

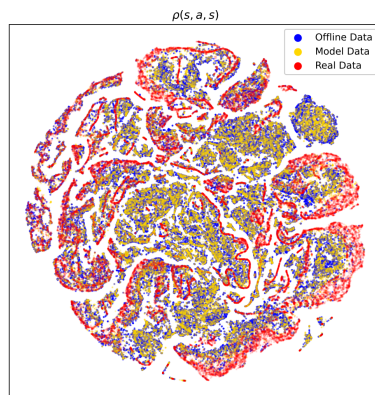


Figure 6. The (s, a, s') distributions generated by SAMBO result in the walker2d-medium-expert task in D4RL benchmark. Model Data represents the distribution of data generated by executing the final learned policy in the dynamic model, while Real Data represents the distribution of data generated by executing the final learned policy in the environment.

We also conducted a visualization experiment on the walker2d-medium-expert dataset within the D4RL benchmark. As shown in Figure 6, SAMBO effectively constrains the Model Data to closely match the Offline Data, and the Real Data generated by executing the learned policy in the actual environment does not significantly deviate from either the Offline Data or Model Data. This highlights the effectiveness of SAMBO in mitigating distribution shift across both benchmarks.

D.2. Detailed Ablation Discussion

SAMBO is regulated by the model bias adjustment coefficient α and the policy shift modification coefficient β .

The model bias adjustment coefficient α controls the degree of adjustment to model-generated data. A larger α leads to excessive conservatism, restricting exploration even in well-performing regions and potentially causing suboptimal

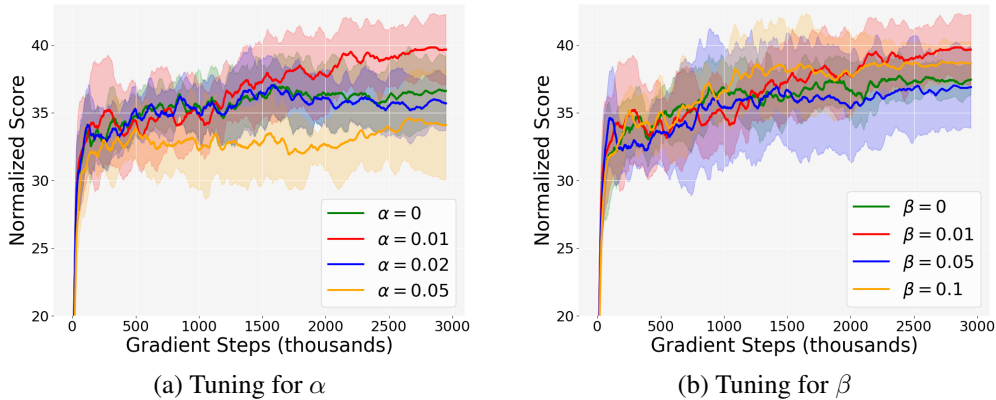


Figure 7. Illustration of hyperparameter experiments in the HalfCheetah-random task in D4RL benchmark.

performance. Conversely, a smaller α may encourage excessive optimism in exploring risky regions, impairing performance. To validate this, we set $\beta = 0.01$ and varied α in the Halfcheetah task. The results, shown in Fig. 7 (a), indicate that both very low ($\alpha = 0$) and high ($\alpha = 0.02$ or 0.05) values lead to decreased performance. Specifically, as α increases from 0 to 0.05, the algorithm initially improves but later declines as it becomes increasingly conservative, which impedes exploration. This underscores that both excessively low and high values of α are detrimental to policy learning.

The policy shift modification coefficient β governs the extent of modification applied to the offline data, thereby influencing the degree of deviation from the behavior policy. A larger β value promotes increased exploratory behavior by encouraging the algorithm to diverge from the behavior policy. However, this also introduces a heightened risk of taking unsafe actions. As shown in Fig. 7 (b), the algorithm exhibits some performance fluctuations as β increases from 0 to 0.1, though it generally maintains robustness. A low value of β may lead to suboptimal solutions, whereas a high value of β can induce excessive aggressiveness of the algorithm, resulting in performance instability. Thus, β should also be set appropriately to balance exploration and stability.

D.3. Performance Compare

We also compared the performance curves of model-based approaches on other tasks in the NeoRL benchmark. The curve for MOBILE was obtained by executing the official implementation. Since MOPO does not have an official implementation on NeoRL, we report its score based on the results presented in the original NeoRL paper.

As shown in Figures 8 to 16, SAMBO outperforms in all Hopper and Walker2d tasks, both of which are more complex and challenging. Although it exhibits slower convergence initially in the Walker2d-M and Walker2d-H tasks, its performance improves rapidly as the experiment progresses, ultimately achieving state-of-the-art (SOTA) levels. On the other hand, SAMBO also demonstrates comparable performance in simpler HalfCheetah tasks.

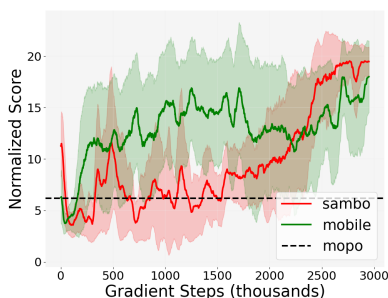


Figure 8. Hopper-L

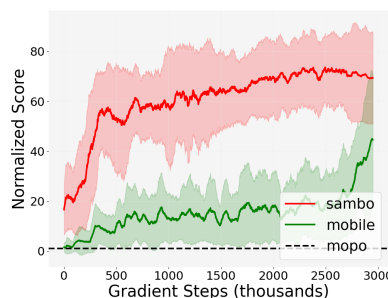


Figure 9. Hopper-M

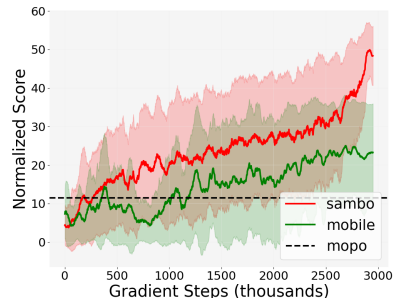


Figure 10. Hopper-H

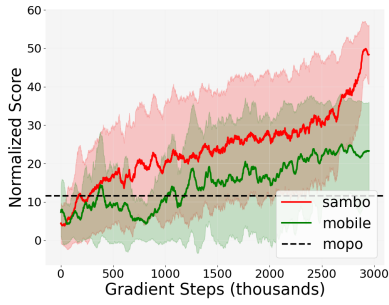


Figure 11. Walker2d-L

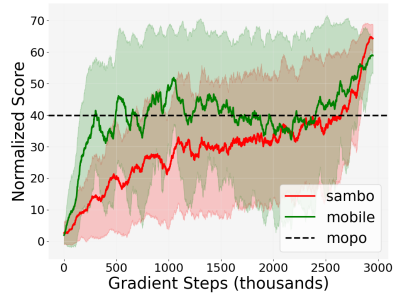


Figure 12. Walker2d-M

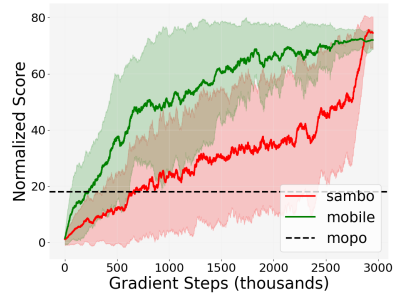


Figure 13. Walker2d-H

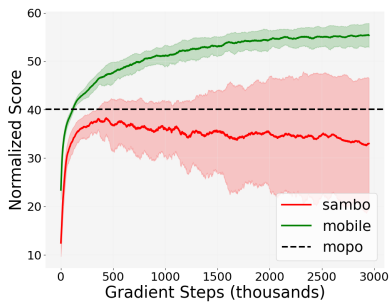


Figure 14. HalfCheetah-L

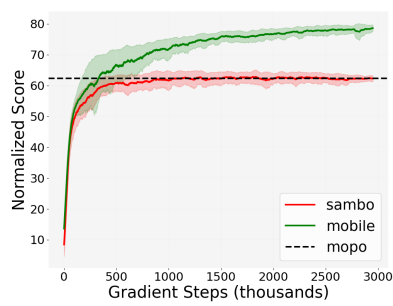


Figure 15. HalfCheetah-M

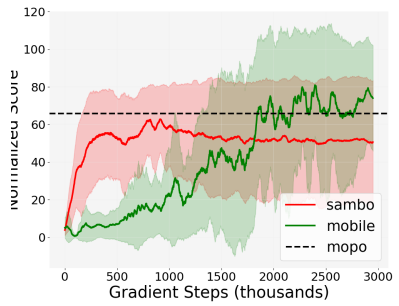


Figure 16. HalfCheetah-H